Published online 20 December 2022

Nucleic Acids Research, 2023, Vol. 51, No. 1 ***29–40***
https://doi.org/10.1093/nar/gkac1193

A versatile and convenient tool for regulation of DNA strand displacement and post-modification on pre-fabricated DNA nanodevices

Yangwei Liao[1,2,†], Hao Hu[1,†], Xiaofeng Tang[1,3,†], Yang Qin[1], Wei Zhang[1], Kejun Dong[1], Bei Yan[1], Yaoqin Mu[1], Longjie Li[1,5,*], Zhihao Ming[1,*] and Xianjin Xiao[1,4,*]

[1]Institute of Reproductive Health, Tongji Medical College, Huazhong University of Science and Technology, Wuhan, 430030, China, [2]Department of Biliary-Pancreatic Surgery, Affiliated Tongji Hospital, Tongji Medical College, Huazhong University of Science and Technology, 1095 Jiefang Ave, Wuhan, 430030, Hubei, China, [3]Prenatal Diagnosis Center, West China Second University Hospital, Sichuan University, Chengdu, Sichuan, 610041, China, [4]Department of Laboratory Medicine, Tongji hospital, Tongji Medical College, Huazhong University of Science and Technology, Wuhan, 430030, China and [5]School of Life Science and Technology, Wuhan Polytechnic University, Wuhan, 430023, China

Received October 17, 2022; Revised November 18, 2022; Editorial Decision November 18, 2022; Accepted December 01, 2022

ABSTRACT

Toehold-mediated strand displacement and its regulatory tools are fundamental for DNA nanotechnology. However, current regulatory tools all need to change the original sequence of reactants, making the regulation inconvenient and cumbersome. More importantly, the booming development of DNA nanotechnology will soon promote the production of packaged and batched devices or circuits with specified functions. Regarding standardized, packaged DNA nanodevices, access to personalized post-modification will greatly help users, whereas none of the current regulatory tools can provide such access, which has greatly constrained DNA nanodevices from becoming more powerful and practical. Herein, we developed a novel regulation tool named Cap which has two basic functions of subtle regulation of the reaction rate and erasability. Based on these functions, we further developed three advanced functions. Through integration of all functions of Cap and its distinct advantage of working independently, we finally realized personalized tailor-made post-modification on pre-fabricated DNA circuits. A pre-fabricated dual-output DNA circuit was successfully transformed into an equal-output circuit, a signal-antagonist circuit and a covariant circuit according to our requirements. Taken together, Cap is easy to design and generalizable for all strand displacement-based DNA nanodevices. We believe the Cap tool will be widely used in regulating reaction networks and personalized tailor-made post-modification of DNA nanodevices.

GRAPHICAL ABSTRACT

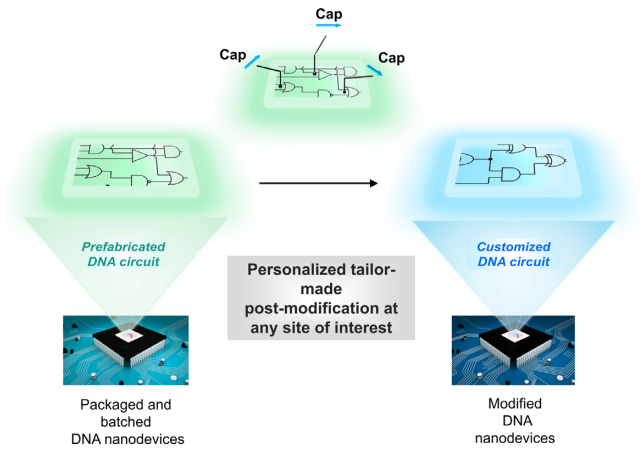

INTRODUCTION

Due to the specificity and programmability of Watson–Crick base pairing (1), DNA is widely used as a basic material for precisely predictable and controllable nanoscale devices (2–8). These DNA-based devices use hydrogen bonds to maintain structural stability (9–11) in the resting state, and use DNA strand displacement reaction networks to

*To whom correspondence should be addressed. Tel: +86 027 8369 2651; Fax: +86 027 8369 2651; Email: xiaoxianjin@hust.edu.cn
Correspondence may also be addressed to Zhihao Ming. Email: zh-ming@hust.edu.cn
Correspondence may also be addressed to Longjie Li. Email: lilongjie@whpu.edu.cn
†The authors wish it to be known that, in their opinion, the first three authors should be regarded as Joint First Authors.

function in operation (12,13). The most primitive DNA strand displacement reaction is only initiated by DNA double-strand end breathing (14,15), which is very slow. Later, in the toehold-based DNA combinatorial displacement model proposed by Yurke *et al*. (6,16), strand displacement was mediated by complementarity in the toehold region, and the reaction rate was greatly enhanced. Based on this model, many toehold-based strand displacement reaction regulators (17–21) have emerged, including remote toehold (22), allosteric toehold (23), wedge-like DNA tools (24), clip toehold (25) and cooperative branch migration (CBM) methods (26). These tools allow subtle regulation of reaction rates which enables the process of different reactions to be accurately controlled within a specified time. On this basis, more advanced functions such as selection of reaction pathways, resetting of the reaction and allosteric strand displacement have been demonstrated. Through integration of the above regulation functions, researchers have further developed various powerful DNA nanomachines. For instance, Weihong Tan constructed the DNA tetrahedron nanostructure (27,28), which can be used to detect and image mRNA in tumor cells. Erik Winfree (29) constructed and designed the concept of the DNA computer (30,31), which can perform calculations such as the cube root (32). In conclusion, large-scale complex DNA nanodevices based on toehold-mediated reaction and its regulatory tools can perform a variety of complicated functions, and have gradually achieved a wide range of applications in the fields of DNA computing (33–35), drug delivery (36–39), molecular diagnosis (40–42) and disease treatment (43–45), which makes it a promising field in DNA nanotechnology.

However, the aforementioned toehold regulation tools all change the traditional toehold-mediated reaction framework to some extent. For example, the remote toehold method (22) adds a spacer region near the toe region. The allosteric toehold (23) introduces a regulator, which splits the strand displacement reaction into a branch migration and a strand displacement reaction. The introduction of clips (25) requires changing the sequence and length of the toe region. CBM methods (26) introduce unpaired domains and Helper strands. Thus, the aforementioned regulation tools for toehold-mediated strand displacement reaction all inevitably alter the original sequence of reactants. Such alterations not only bring more complexity and less compatibility to the sequence and structural design, but, most importantly, they completely block the possibility of post-modification of DNA nanodevices that have been built or packaged. The booming development of DNA nanotechnology will soon promote the production of integrated, packaged and batched devices or circuits with specified functions. Regarding standardized packaged DNA nanodevices, access to personalized post-modification will be of tremendous help to users, whereas none of the current regulatory tools can provide such access, which has greatly constrained DNA nanodevices from becoming more powerful and practical.

Herein, we designed a novel regulation tool based on four-way strand displacement. On the basis of a conventional toehold-mediated reaction, a single-stranded regulation tool, called 'Cap', is introduced (Figure 1). The Cap strand was designed to be complementary to the invading strand, and according to the sequence relationship in the input strand (denoted as I-strand), template strand (denoted as T-strand) and output strand (denoted as O-strand), the Cap strand would also be complementary to the output strand. Consequently, during the strand displacement process, the Cap strand would dissociate from the I-strand and immediately hybridize with the O-strand, forming a four-way strand displacement. The regulatory functions of the Cap strand originate from the much slower kinetics of the four-way strand displacement process than the conventional three-strand toehold-mediated reaction. As was demonstrated in previous literature (13), the Cap strand should be able to regulate the strand displacement rate by adjusting its length: the longer of the Cap strand, the slower the reaction rate. However, such regulation was very rough: the reaction rate dropped sharply when the Cap strand was lengthened by only ∼5 nt. Therefore, here in this work, we wanted to establish a much more subtle regulation tool. Toward a fixed length of Cap, we came up with incorporating bulges to change the stability of the Cap/input duplex. The mechanism by which the bulge would affect the stability or thermodynamics of the Cap/input duplex was that the bulge could change the sequence and spatial structure of the duplex. Since the bulge does not alter the number of paired bases of the Cap/input duplex, we assume its influence on the reaction rate would be mild and subtle. Overall, the proposed Cap was a multilevel regulation tool for DNA strand displacement. In brief, we could quickly adjust the reaction rate to a certain range by changing the length of the Cap and then subtly tune the rate close to the desired value by changing the bulge. We also could adjust the concentration of the Cap to change the degree of reaction. Moreover, a few additional nucleotides can be designed at the end of the Cap so that it is able to be retrieved by adding complementary (c-Cap) strands and thereby execute erasability. Furthermore, taking advantages of the wide range of reaction rates and erasability, the Cap tool possesses more advanced regulation functions such as subtle distribution of reaction paths, selective activation and a sliding rheostat. Most importantly, all of the regulatory functions can be accomplished by the Cap strand alone, without changing the sequence and structure of the original toehold-mediated reaction at all, making the Cap strand a perfect and powerful tool for realizing personalized tailor-made post-modification on packaged and batched DNA nanodevices.

MATERIALS AND METHODS

Materials

ThermoPol reaction buffer was purchased from New England Biolabs (Ipswich, MA, USA). DNA strands were synthesized and purified by high-performance liquid chromatography (HPLC; Sangon Biotech Co., Shanghai, China). The sequences of all the probes and targets that used in this work are summarized in Supplementary Tables S1–S9.

Methods

Subtle regulation of the toehold-mediated reaction rate. The reaction system consists of associated DNA strands, ddH_2O and ThermoPol reaction buffer, and the total volume was 50 μl. For detailed manual procedures: firstly, the T-strand and O-strand were heated at 85°C for 1 min, lowered to 55°C for 1 min and then incubated at 37°C for 30 min to form a complementary double-stranded structure. Then, the I-strand and Cap were added to the system. The concentrations of I-strand, Cap, T-strand and O-strand were all 100 nM. The fluorescence was measured in a microplate reader (BioTek, USA). Instrument parameters are set as follows: excitation wavelength, 485 nm; emission wavelength, 528 nm; gain level, 90; detection time, 2 h.

Erasability. The preparation of solutions and measurement procedures are the same as described above before the c-Cap strand was added. For erasability of Cap, 100 nM of c-Cap was added at timepoint of 40 min and the fluorescence was contineously measured for 2h.

Subtle distribution of reaction pathways. The reaction system consists of appropriate amount of associated DNA strands, ddH_2O and ThermoPol reaction buffer, and total volume was 50 μl. For detailed manual procedures: firstly, M1 and Template 1, M2 and Template 2, Y1 and Template 3, Y2 and Template 4 were heated at 85°C for 1 min, lowered 55°C for 1 min and then incubated at 37°C for 30 min to form complementary double-stranded structures, separately and respectively. Then, those formed duplexes, X and Cap 1/Cap 2 were added to the system. The concentrations of all the DNA strands in the reaction system were 100 nM. The fluorescence was measured in a microplate reader (BioTek, USA). Instrument parameters are set as follows: excitation wavelength of FAM, 485 nm; emission wavelength of FAM, 528 nm; excitation wavelength of HEX, 535 nm; emission wavelength of HEX, 556 nm; gain level, 90; detection time, 2 h.

Selective activation. The reaction system consists of appropriate amount of associated DNA strands, ddH_2O and ThermoPol reaction buffer, and the total volume was 50 μl. For detailed manual procedures: firstly, c-Cap 3A, c-Cap 3B, c-Cap 3C, Template 3A, Template 3B, Template 3C, Output 3A, Output 3B and Output 3C were added. Then, Input 3A and Cap 3A, Input 3B and Cap 3B, Input 3C and Cap 3C, Output 3A and Template 3A, Output 3B and Template 3B, Output 3C and Template 3C were heated at 85°C for 1 min, lowered to 55°C for 1 min and then incubated at 37°C for 30 min to form complementary double-stranded structures, separately and respectively. Finally, those formed Input 3A/Cap 3A duplex, Input 3B/Cap 3B duplex, and Input 3C/Cap 3C duplex were added to the system at timepoint of 9, 66 and 101 min, respectively and sequentially. The concentrations of all the DNA strands in the reaction system were 100 nM. The fluorescence was measured in a microplate reader (BioTek, USA). Instrument parameters are set as follows: excitation wavelength, 485 nm; emission wavelength, 528 nm; gain level, 90; and detection time, 2 h and 40 min.

Slide rheostat. The reaction system consists of appropriate amounts of associated DNA strands, ddH_2O and ThermoPol reaction buffer, and the total volume was 50 μl. For detailed manual procedures: firstly, Input M-2 and Template M-1, Input M-3 and Template M-2, Output and Template M-3, Input S-2 and Template S-1, Cap 4C and Template S-2 were heated at 85°C for 1 min, lowered to 55°C for 1 min and then incubated at 37°C for 30 min to form complementary double-stranded structures, separately and respectively. Then, those formed duplexes were mixed together. Finally, Input M-1, Input S-1, Cap 3A and Cap 3B were added to the system. The concentrations of all the DNA strands excluding the Cap 3A in the reaction system were 200 nM. The concentration of the Cap 3A can be 50, 100, 150 or 200 nM according to the design of different experiments. The fluorescence was measured in a microplate reader (BioTek, USA). Instrument parameters are set as follows: excitation wavelength, 485 nm; emission wavelength, 528 nm; gain level, 90; detection time, 33 min.

Personalized, tailor-made post-modification on packaged, pre-fabricated DNA circuits. The reaction system consists of appropriate amount of associated DNA strands, ddH_2O and ThermoPol reaction buffer, and the total volume up was 50 μl. For detailed manual procedures: firstly, Input 1-2 and Template 1-1, Input 1-3 and Template 1-2, Output 1 and Template 1-3, Input 2-3a and Template 2-2a, Input 2-3b and Template 2-2b, Output 2 and Template 2-3a, Output 3 and Template 2-3b, Template 2-1, Input M and Input 2–2 were heated at 85°C for 1 min, lowered to 55°C for 1 min and then incubated at 37°C for 30 min to form complementary double-stranded or triple-stranded structures, separately and respectively. Then, those formed duplexes and triplexes were mixed together. Cap 5A, Cap 5B, Cap 5C and Cap 5D were added to the system, and their concentrations vary from 20 to 200 nM according to the purpose of post-modification. Finally, Input 1-1a, Input 1-1b, Input 2-1a, Input 2-1b, Cap I1 and Cap I2 were added to the system to initiate the circuit. The concentrations of all the DNA strands excluding Cap 5A, Cap 5B, Cap 5C and Cap 5D in the reaction system were 200 nM. The fluorescence was measured in a microplate reader (BioTek, American). Instrument parameters are set as follows: excitation wavelength, 485 nm; emission wavelength, 528 nm; gain level, 90; detection time, 99 min.

RESULTS AND DISCUSSION

Subtle regulation of the toehold-mediated reaction rate

We firstly investigated the regulation capability of Cap toward the toehold-mediated reaction rate. As illustrated in Figure 1A, we designed and synthesized Input (denoted as I-strand), Template (denoted as T-strand), Output (denoted as O-strand) and various Caps. Using the incorporated bulge as the marker, a Cap strand could be divided into domains X, Y and Z. Domain X and domain Z were designed to be complementary to the I-strand. We then could use a set of variables (X, Y, Z) to denote the Cap, where X is the number of bases spaced from the 3′ end of the Cap to the 3′ end of the bulge, Y is the number of bases in the bulge and Z is the number of bases spaced from

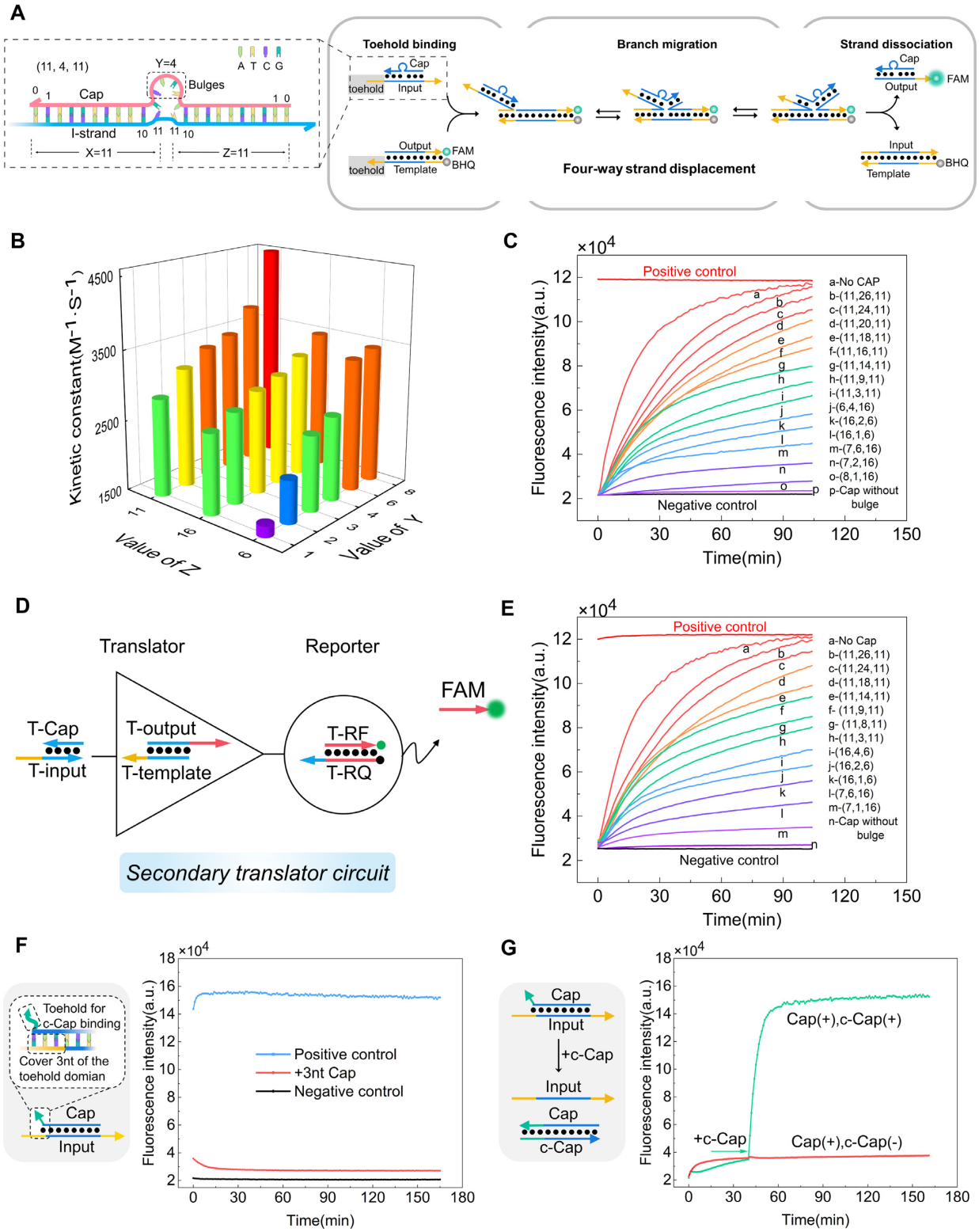

Figure 1. (**A**) Schematic illustration of Cap and the four-way strand displacement process. (**B**) Kinetic constants of the reactions of the 100 nM I-strand invading the 100 nM T-strand/O-strand duplex under the regulation of the 100 nM Cap. For each reaction, different Caps were used, in which Z could be 6, 16 or 11, and Y varied from 1 to 8. (**C**) The fluorescent curves of reactions of the 100 nM I-strand invading the 100 nM T-strand/O-strand duplex under the regulation of 100 nM different Caps. (**D**) Schematic illustration of the secondary translator circuit in which the reaction rate of the first-layer translator is controlled by the Cap strand. (**E**) The fluorescent curves of the secondary translator circuit under the regulation of different Caps. The strands used in the experiment were all fixed at 100 nM. (**F**) A Cap, namely +3 nt Cap, that contains a 10 nt extra sequence and its complementary region with the input strand, covers the whole branch migration domain and three nucleotides of the toehold domain. The toehold-mediated reaction rate controlled by +3 nt Cap is similar to that of the negative control. (**G**) Erasability of the Cap. c-Cap was added at 40 min. Reaction set up: all strands were fixed at 100 nM.

the 5′ end of the CAP to the 5′ end of the bulge. Therefore, the Cap strand depicted in Figure 1A should be denoted as (11, 4, 11). We then investigated the effect of different Caps on the toehold-mediated reaction rate. Figure 1B and Supplementary Figure S1 are the comparison of the kinetic constants of experimental groups in which the value of Z or Y is the same; the corresponding reaction curves and the calculation of kinetic constants can be seen in the Supplementary Data (2.1 and 2.2). From the above results, we could deduce the empirical rules regarding the influence of the location and size of the bulge on the reaction rate: (i) when the size of the bulge (Y) was fixed, the reaction rate with Caps where X = 11 was faster than those with Caps where X = 6 or X = 16, which indicates that the bulge located in the middle of the Cap would make a weaker difference to the reaction rate; and (ii) when the location of the bulge (X and Z) was fixed, the larger the bulge, the faster the reaction rate, which matched the expectation that the Cap/Input duplex was more unstable with a larger bulge.

After determining the basic rules, subtle regulation of the strand displacement reaction rate could be achieved by continuously adjusting the values of X, Y and Z. As shown in Figure 1C and Supplementary Figure S2a, the toehold-mediated reaction rate could be regulated at full range, from 0% to ∼100%. Furthermore, we randomly designed another set of toehold strands and tested the regulation function of the Cap strand. As shown in Supplementary Figure S3, the Cap strand also finely and subtly regulated the reaction rates, demonstrating the generality of the subtle regulation function of the Cap strand (Supplementary Figure S3). We also designed a secondary translator circuit and, by using the Cap strand to control the reaction rate of the first-layer translator, we successfully subtly regulated the reaction rate of the whole secondary circuit (Figure 1D, E; Supplementary Figure S2b), demonstrating the functionality of the Cap strand in multilayer circuits.

We would also like to emphasize that the regulation capability of our proposed Cap toward the toehold-mediated reaction rate is comparable with previously reported regulation tools, but Cap has a distinct and unique advantage over others: the regulation was accomplished only by adding a CAP strand, without changing the structure and sequence of the original toehold-mediated reaction at all. To the best of our knowledge, our proposed Cap has the highest simplicity and convenience among all reported strategies.

Erasability

We then introduced a few additional nucleotides to the end of the Cap strand, and these extra sequences could serve as a toehold region for the complementary c-Cap strand to erase the Cap strand, thereby restoring the reaction to the conventional strand displacement mode. As shown in Figure 1F, we designed a Cap (+3 nt Cap) that contained a 10 nt extra sequence and its region complementary to the Input strand covered the whole branch migration domain and 3 nt of the toehold domain. More experimental results can be seen in Supplementary Figure S4. As expected, the Cap strand almost blocked the strand displacement process, rendering a very low fluorescent signal (the red curve in Figure 1G). We then added c-Cap (+3 nt c-Cap) to erase the Cap strand, and the toehold-mediated reaction was released, producing a strong signal (the green curve in Figure 1G).

Overall, we have demonstrated two basic functions of Cap: subtle regulation of the reaction rate and erasability. We then endeavored to integrate the basic functions of Cap and developed three advanced functions with specific utility: (i) subtle distribution of reaction pathways; (ii) selective activation; and (iii) a slide rheostat.

Subtle distribution of reaction paths

We firstly developed the function of selecting and distributing reaction pathways for the Cap. As shown in Figure 2A, we designed two parallel secondary strand displacement pathways. According to the sequence design, input X was able to enter both ways. When entering pathway 1 (invading Template 1), the output M1 strand would invade fluorescently FAM-labeled Template 3 and emit green fluorescent signals. On the other hand, when entering pathway 2 (invading Template 2), the output M2 strand would invade HEX-labeled Template 4, emitting red fluorescent signals at another wavelength. We then designed two Caps. Cap 1 was complementary to the tail domain (colored in yellow) of M1, while Cap 2 was complementary to the tail domain (colored in green) of M2. As shown in Figure 2B, we could use Caps to select and distribute reaction pathways. If we only add a long Cap 1, the process of M1 invading Template 3 would be blocked. Since the reactions of input X invading Template 1/2 were reversible (the length of the toehold domain was identical to that of the dissociation domain), the input X that had entered pathway 1 but was blocked at the second step would be retrieved and enter pathway 2 following Le Chatelier's principle. Likewise, if we only add long Cap 2, the whole reaction would be pushed into pathway 1. Furthermore, we could change the length of the added Caps or incorporate bulges into the Caps to subtly control the distribution of the two pathways. We then synthesized Cap 1-L/Cap 2-L with large bulges (8 nt), Cap 1-M/Cap 2-M with medium bulges (4 nt) and Cap 1-S/Cap 2-S with small bulges (2 nt), and used these Caps to control the reaction pathways. It was worth noting that the lengths of domains X and Z were fixed at 7 nt and 8 nt, and the concentration was fixed at 100 nM for all Caps. As shown in Figure 2C and E, when no Caps were added, input X would evenly enter two pathways, producing a median fluorescent signal between the positive control and negative control. When adding Cap 1 strands, the green signal became weaker and the red signal became stronger as the bulges of Cap 1 shrunk, indicating that input X entered less into pathway 1 but more into pathway 2. In contrast, when adding Cap 2 strands, the green signal became stronger and the red signal became weaker as the length of Cap 2 increased, indicating that input X entered more into pathway 1 and less into pathway 2. Comparing the plateaued fluorescence intensities, we could calculate the percentage of input X entering pathway 1 and pathway 2. As shown in Figure 2D and F, the calculated percentages varied gradually and mildly from nearly 0% to 100%, demonstrating that the Cap tool was able to subtly control the distribution of reaction pathways. Moreover, such control was extremely convenient, just adding an additional

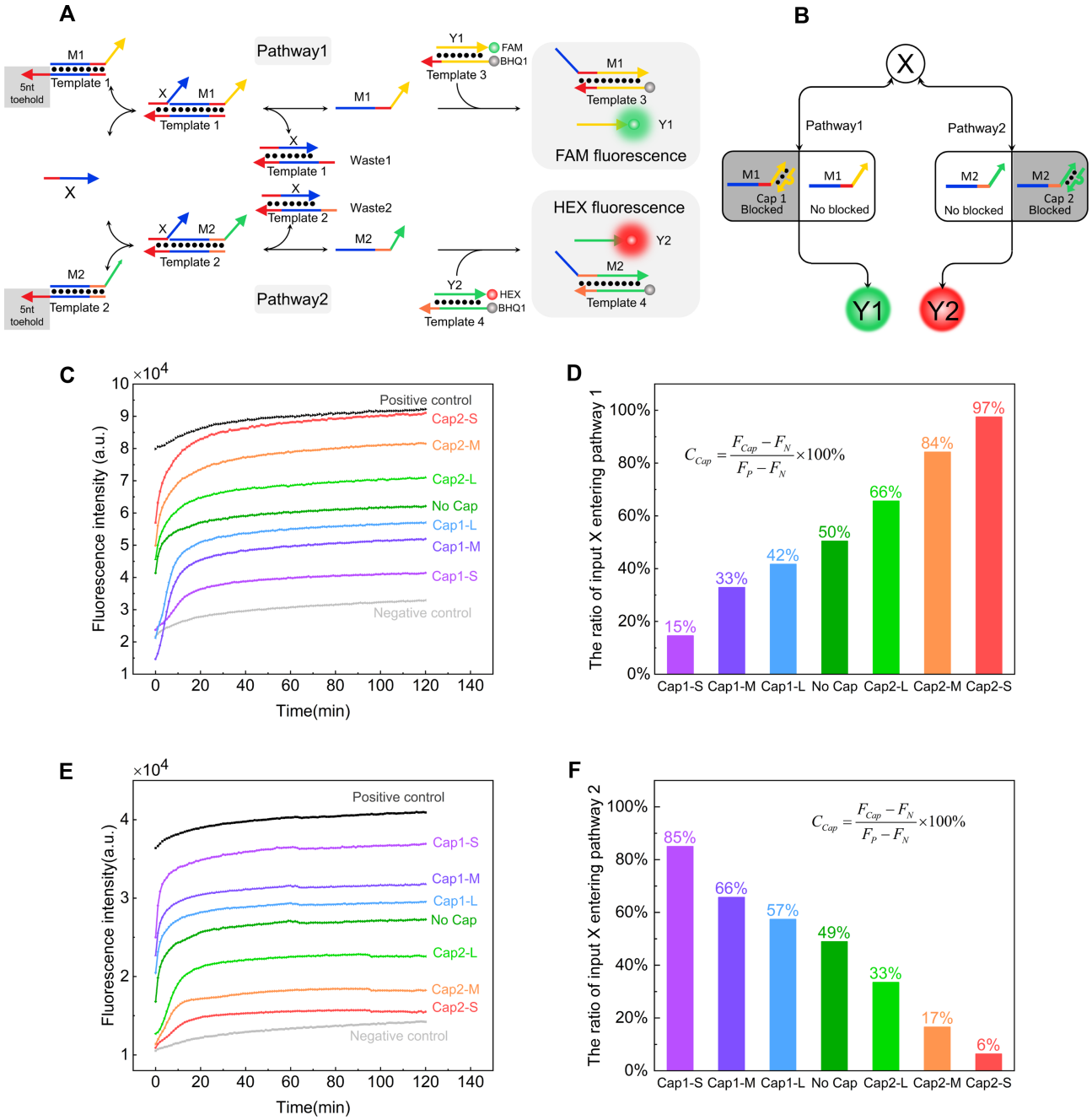

Figure 2. (**A** and **B**) Schematic illustration of the advanced function of the Cap: subtle distribution of reaction pathways (A). Cap 1 and Cap 2 bind with M1 and M2, respectively, to achieve the distribution of reaction pathways (B). (**C**) The FAM fluorescent curves of the two-pathway circuit under the control of different Caps. (**D**) The ratio of input X entering pathway 1 calculated from (C). The equation for calculation is shown in the inset, where C_{Cap} is the ratio to be calculated, F_{Cap} is the plateau value of the fluorescent curves in (C), and F_p and F_N are the plateau values of the fluorescent curves of the positive and negative controls in (C), respectively. (**E**) The HEX fluorescent curves of the two-pathway circuit under the control of different Caps. (**F**) The ratio of input X entering pathway 2 calculated from (E). The equation for calculation is shown in the inset and is the same as that in (D). Reaction set up: all strands were fixed at 100 nM.

strand and without changing the sequence or concentration of the original strands at all.

Selective activation

We then tried to develop the function of selective activation for the Cap tool. As shown in Figure 1D, the reaction rate of a toehold strand displacement process could be adjusted from very fast to almost zero simply by using different Cap strands, and such a transition of reaction rate resembled the on and off state of a switch. Taking advantage of the erasability of Cap, we could achieve switching of the on and off state in a multiplexed mode, namely selective activation. Here in the experiment, we designed three

sets of toehold-mediated reaction species, each of which included input (Input 3A–3C), template (Template 3A–3C), output (Output 3A–3C), Cap (Cap 3A–3C) and reporters (RF labeled with FAM and RB labeled with HEX). All of the strands were added into one tube to form a triplex reaction system. Since the Caps were designed to be long enough, the toehold-mediated reactions were all blocked at the initial stage. We then could add different c-Caps (c-Cap 3A, c-Cap 3B abdc-Cap 3C) to selectively activate the corresponding toehold-mediated reaction. As shown in Figure 3A, to each tube, we added three sets of templates and outputs. Then, to those tubes, we added eight combinations of c-Caps that covered all possible situations to potentially activate different toehold-mediated reactions. As a result, when Input-Cap dsDNA 3A, 3B and 3C were sequentially added, the fluorescence curves in Figure 3B presented different shapes as we expected, demonstrating the functionality of selective activation. We would also like to note that from the perspective of biosensing or nucleic acid analysis, the selective activation could also be utilized for multiplexed detection. For instance, in the above experiment, the c-Caps could be regarded as analytes and, according to the shapes of the fluorescence curves, we could determine the compositions of the analytes, which is exactly the meaning of multiplexed detection.

Slide rheostat

Additionally, we could evolve the Cap tool for a more advanced and powerful function: regulating as a slide rheostat. We used the term‘slide rheostat’ as a vivid analogy to show that the Cap can provide convenient and ‘smooth’ regulation to the process and the output yield of reactions. As illustrated in Figure 4A, the main reaction pathway was a tertiary strand displacement process (Supplementary Figures S5 and S6 show the basic functionality of the main reaction pathway). Toward the second toehold-mediated reaction, we designed a Cap (Cap 4A) to hybridize with Input M-2 and thereby subtly regulated its proportion of entering the third layer of the circuit. Analogously speaking, Cap 4A played the role of a slide rheostat in the electronic circuit: longer or higher concentration of Cap 4A could impose greater resistance to the reaction pathway and rendered a lower ‘current’ of the whole circuit. More importantly, the Cap-based slide rheostat could be further scaled up. As shown in Figure 4A, apart from the main reaction pathway, we designed a side reaction pathway consisting of two layers of the strand displacement process. The final output of the side reaction pathway was Cap 4C, which was long enough to block Input M-3 from initiating the third toehold-mediated reaction of the main pathway. Also, in the side reaction pathway, a Cap 4B strand was loaded on Input S-2, and thereby the output (Cap 4C) concentration of the whole two-layer side reaction pathway could be subtly controlled by a Cap (Cap 4B). Collectively, Cap 4B determined the amplitude of resistance imposed on the main reaction and thereby further determined the overall output signal. Since the length and bulge of the Cap 4B strand could be flexibly adjusted, the side reaction pathway as a whole functioned as a slide rheostat, and Cap 4B was the slider. Experimental results shown in Figure 4B demonstrated our design: when no Cap 4B strand was added, the main reaction pathway was largely blocked, exhibiting low fluorescence signal. When different Caps were added, the output signal was increased by different amounts, demonstrating that the side reaction as a whole could perform as the slide rheostat to adjust the main reaction pathway. Furthermore, we could simultaneously adjust the simple and scalable slide rheostat to achieve more powerful control of the DNA circuit. As was shown in Figure 4C–F, by using different combinations of Cap 4A and Cap 4B, the normalized yield of output varied from 0 to 1 subtly. It is worth noting that the function of a slide rheostat also revealed that the Cap strand could provide a convenient way for constructing cross-talk among different pathways or circuits. Collectively, we have integrated the fine rate-regulating capability of Cap into a more complexed DNA circuit and constructed a DNA slide rheostat at both a simple and a scalable level. We would also like to point out that the function of a slide rheostat revealed that the Cap strand could provide a convenient way for constructing cross-talk among different pathways or circuits.

Personalized, tailor-made post-modification on packaged, pre-fabricated DNA circuits

Overall, we have demonstrated two basic functions of Cap (subtle regulation of the reaction rate and erasability) and three advanced functions with specific utility (subtle distribution of reaction pathways, selective activation and slide rheostat). Based on the exceptional property of functioning independently of the Cap, all of the above functions could be imposed on a DNA circuit at any time, whether at the design step or post-modification on an existing circuit, without changing the sequence and structure of the original circuit at all. As shown in Figure 5A, toward a packaged large-scale DNA circuit, we could select any site of interest and apply Cap strands to reorganize the reaction pathway and, finally, the pre-fabricated DNA circuit could be post-modified and transformed into executing personalized tailor-made functions.

To comprehensively exhibit this powerful capability of the Cap tool, a relatively complex DNA circuit was designed and pre-fabricated, and, by adding different Cap/c-Cap strands, all three advanced regulatory functions were imposed on the pre-fabricated circuit, endowing it with completely different computation modes. As shown in Figure 5B, the circuit designed by us has three tertiary reactions. The first layer of the reaction pathway 1 was an OR gate, and its final output was Output 1 which was labeled by FAM. Reaction pathways 2 and 3 shared the same first layer which was an AND gate. The Input 2-2 produced by the first layer of pathway 2 had an equal chance of entering the second layers of pathways 2 and 3. The final output of pathway 2 was Output 2, which was designed to be the Cap of the input strand (Input 1-3) for the third layer of pathway 1; therefore, it could inhibit the third-layer reaction and the final output signal of pathway 1. The final output of pathway 3 was Output 3, which was labeled by HEX. In addition to the basic reaction framework, we also designed Cap I1 to inhibit Input 1-1a and Input 1-1b, and Cap I2 to inhibit Input 2-1a so that the initial leakage of the pre-fabricated DNA circuit was silenced. Taking advantage of the selective

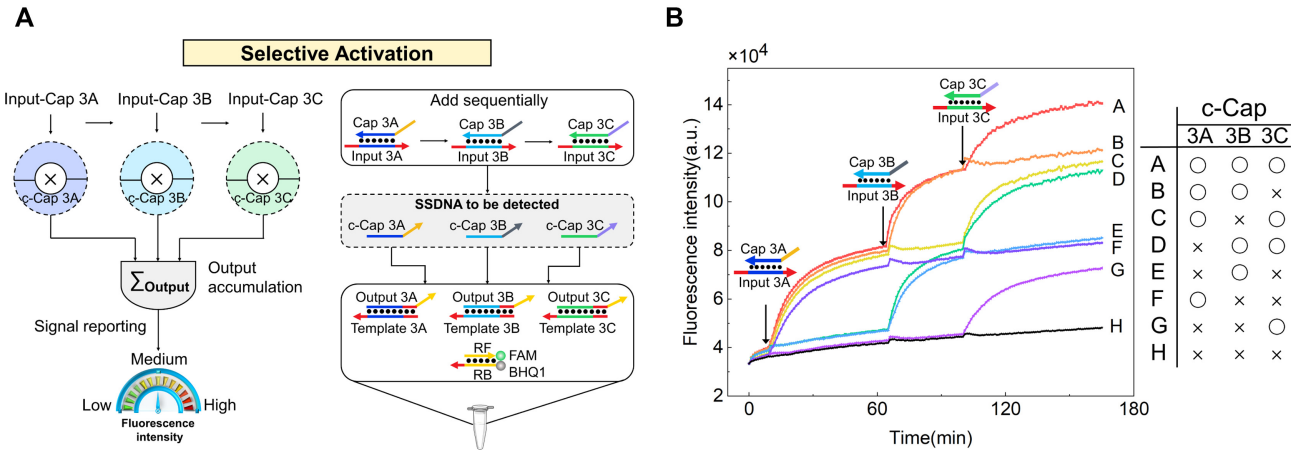

Figure 3. (**A**) Schematic illustration of the advanced function of Cap: selective activation. (**B**) The fluorescent curves of reactions with different Inputs and Caps. Input 3A and Cap 3A, Input 3B and Cap 3B, and Input 3C and Cap 3C were added to the system at 9 min, 66 min and 101 min, respectively and sequentially. Reaction set up: all strands were fixed at 100 nM.

activation property of the Cap tool, c-Cap I1 and c-Cap I2 could be added at any time to initiate the operation of the whole circuit. Comprehensively, we actually built a DNA circuit that mixed a digital logic circuit and an analog circuit. The first-layer OR gate and AND gate for Input 1-1 and Input 2-1 at the beginning determined whether there would be an output signal. The second and third layers of the circuit were actually analog circuits which tuned the amplitude of the output signal. The powerful capability of the Cap allows it not only to selectively activate the logic circuit but also to reprogram the analog circuit for outputting signals with different amplitudes.

Based on the above reaction framework, we firstly verified the logical performance of this circuit, and the experimental results were in accordance with the truth table (Supplementary Figure S7). Then, we focused on applying post-modification to the analog part of the pre-fabricated circuit by adding Cap strands at four designated positions. In these experiments, all four primary inputs (Input 1-1a, Input 1-1b, Input 2-1a and Input 2-1b) were added and the logical outputs of the FAM channel and HEX channel should both be '1'. However, we could add different Caps at various positions to make the amplitudes of logical '1' completely different. As shown in Figure 5B, Cap 5A, Cap 5B, Cap 5C and Cap 5D were designed to be complementary to Input 2-3b, Input 2-3a, Input 2-2 and Input 1-2, respectively. When different amounts of either Cap 5A or Cap 5B were added, the distribution of reaction pathways of Input 2-2 could be subtly controlled: when Cap 5A was added, pathway 3 was inhibited and the HEX signal was reduced. Simultaneously, the output of pathway 2 was increased, which led to a stronger inhibition of pathway 1 and, ultimately, a simultaneous decrease in the FAM signal was observed. The opposite variation occurred with the addition of Cap 5B, where the FAM and HEX signals increasing simultaneously. Further, since Cap 5A and 5B could act as a sliding rheostat, the final signal range could be manipulated by controlling the amount of these Caps added. For instance, we could add an appropriate amount of Cap 5A and 5B to make 'Output 1 (FAM) = Output 3 (HEX)' and their values ranged from 0 to 1 as regulated. Overall, through post-modification by Cap 5A and Cap 5B, we have transformed the original dual-output circuit into an equal-signal output circuit with any adjustable intensity (Figure 5C–E). On the other hand, we could also transform the original circuit into a signal-antagonist circuit: when Cap 5C was added, pathways 2 and 3 were both inhibited, and the circuit behaved as an increase in the FAM signal and a decrease in the HEX signal (Figure 5F). When Cap 5B and Cap 5D were added, pathway 1 and pathway 2 were inhibited, and the circuit showed a decrease in FAM signal and an increase in HEX signal (Figure 5F). Under both antagonistic modes, the formula 'Output 1 (FAM) + Output 3 (HEX) = Constant' applied (Figure 5G), and this constant value could also be adjusted to any number between 0 and 1. Further, when Cap 5A and Cap 5C, or Cap 5B and Cap 5C were added, paths 2 and 3 were inhibited to different extents (Figure 5I, J), and the circuit behaved as Output 1 (FAM) = k × Output 3 (HEX). This k value could be changed to any number (in Figure 5K, k was set to be 2). Further, when Cap 5A and Cap 5C or Cap 5B and Cap 5C were added, pathway 2 and pathway 3 were inhibited to different degrees (Figure 5H, I), and the circuit behaved as Output 1 (FAM) = k × Output 3 (HEX), where the parameter k could be adjusted arbitrarily (in Figure 5J, k was set to be 2).

In a word, we have achieved personalized and tailor-made post-modification of pre-fabricated DNA circuits simply by adding different kinds and concentrations of Cap strands to the system, endowing the original DNA circuit with completely new computation functions.

CONCLUSION

In conclusion, we have developed a novel tool for regulating DNA strand displacement reactions: the Cap. By adjusting the length of the Cap and the size and position of the bulge incorporated within it, we could easily achieve subtle regulation of the reaction rate. In addition, by designing a few extra nucleotides at the end of the Cap, its erasability was accomplished. Based on the above two basic properties of Cap, we further developed three advanced functions with specified utility: subtle distribution of reaction path-

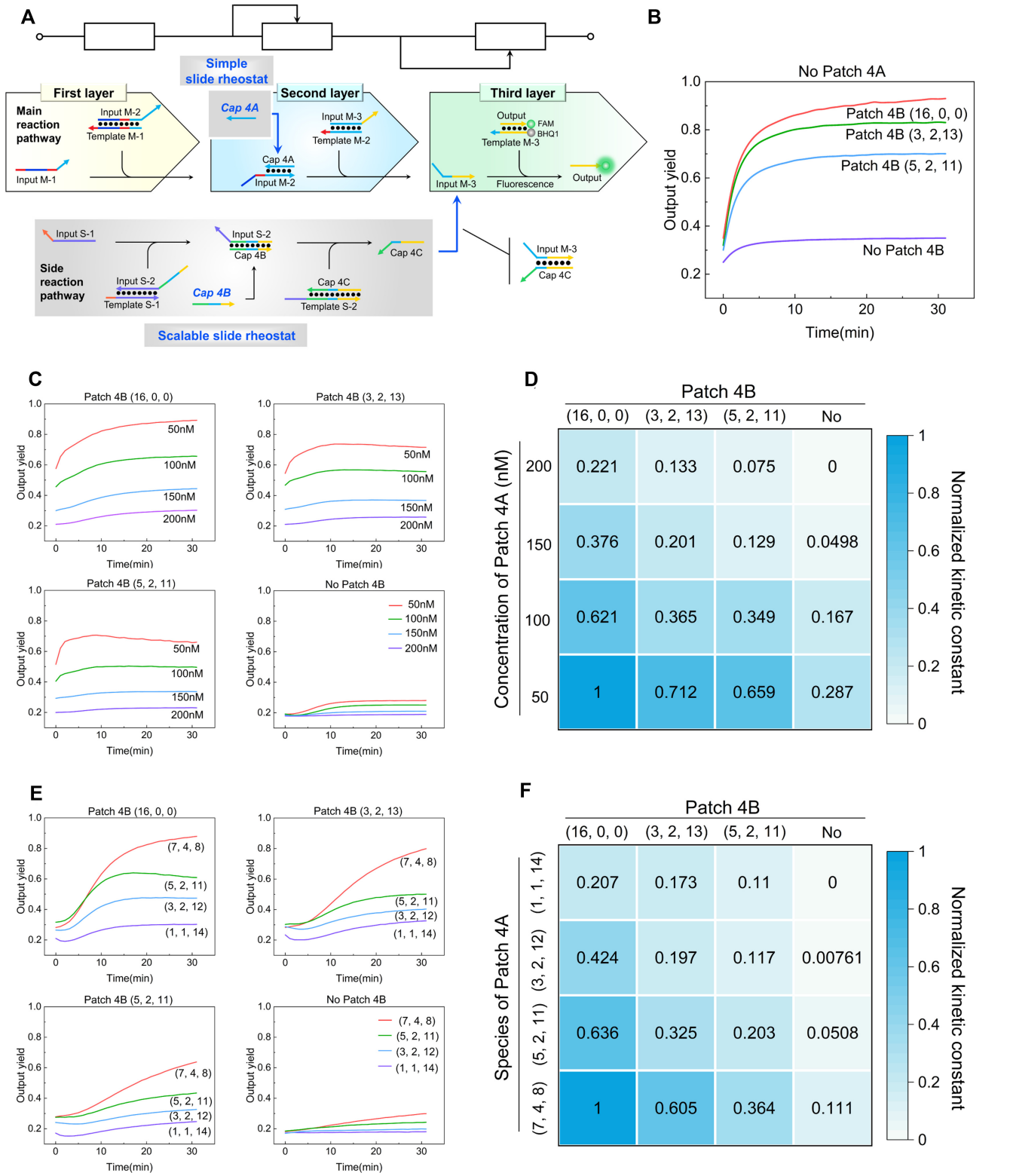

Figure 4. (**A**) Schematic illustration of the advanced function of Cap: slide rheostat. Cap 4A function as a simple slide rheostat. The side reaction pathway as a whole functions as a scalable slide rheostat. (**B**) The fluorescent curves of the tertiary circuit of (A) under the regulation of different Cap 4B strands. (**C** and **D**) The fluorescent curves (C) and normalized kinetic constants (D) of the tertiary circuit of (A) under the regulation of Cap 4B strands with different sequences and the Cap 1 strand with different concentrations. (**E** and **F**) The fluorescent curves (E) and normalized kinetic constants (F) of the tertiary circuit of (A) under the regulation of both Cap 4A and Cap 4B strands with different sequences. Reaction set up: except for Caps, all other strands were fixed at 200 nM. The concentrations of Caps were determined according to the purpose of the experiment.

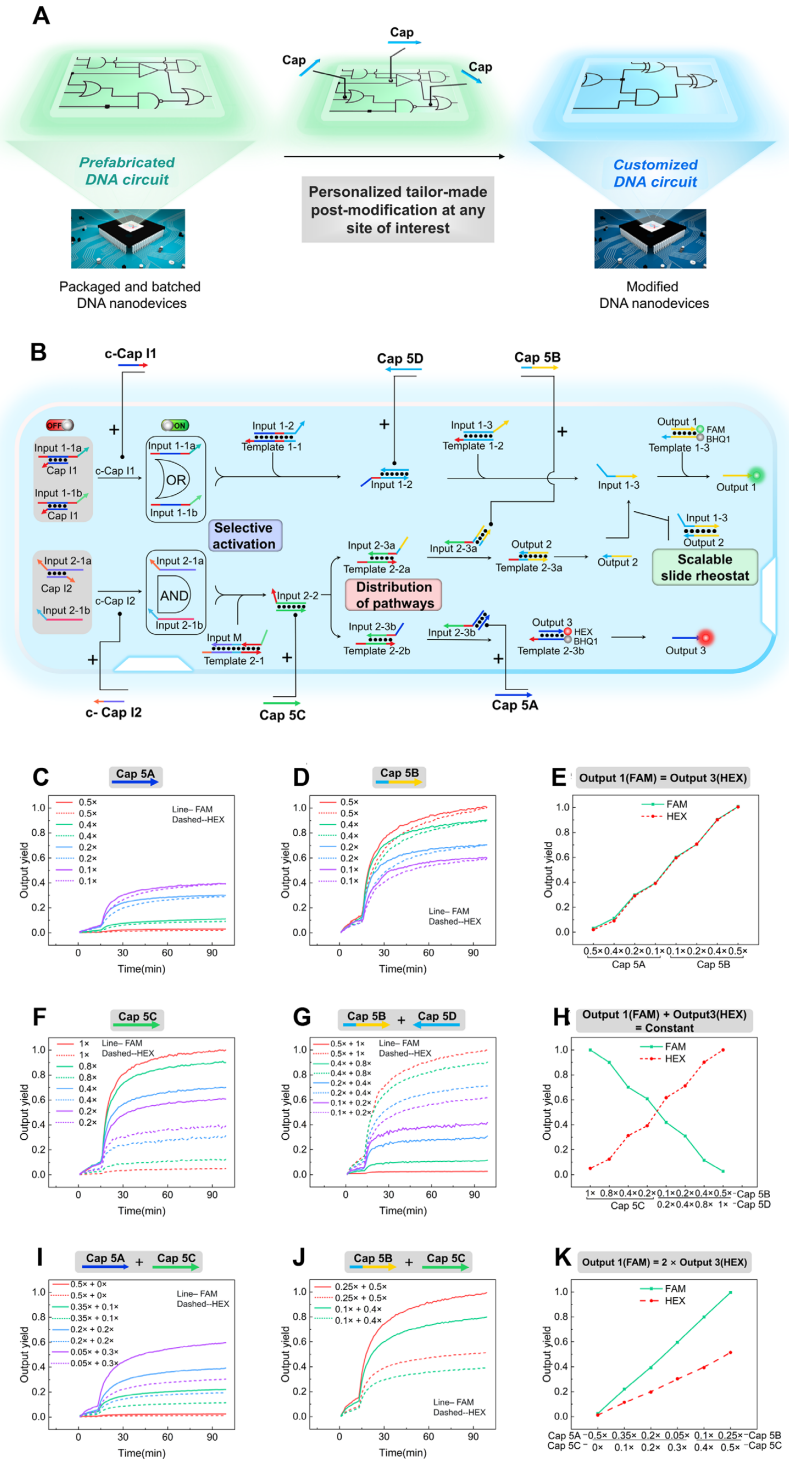

Figure 5. (**A**) Schematic illustration of the Cap-based post-modification on packaged, pre-fabricated DNA circuits. (**B**) A pre-fabricated complex DNA circuit that integrated all regulatory functions of Cap. Four sites are reserved for Caps to execute personalized, tailor-made post-modification. (**C** and **D**) The fluorescent curves of the circuit of (B) under the modification of Cap 5A (C) and Cap 5B (D). The line and dashed curves of '0.5×' describe the output yield of Output 1 labeled as FAM and Output 3 labeled as HEX in the reaction with 0.5× 200 nM Cap 5A, respectively. The meanings of other annotations in (C), (D) and (F) are similar. (**E**) The output yield calculated from the plateau values of curves in (C) and (D), showing Output 1 (FAM) = Output 3 (HEX). (**F** and **G**) The fluorescent curves of the circuit of (B) under the modification of Cap 5C (F) and Cap 5B, 5D (G). The line and dashed curves of '0.5× + 1×' describe the output yield of Output 1 labeled as FAM and Output 3 labeled as HEX in the reaction with 0.5× 200 nM Cap 5B and 1× 200 nM Cap 5D. The meanings of other annotations in (G), (I) and (J) are similar. (**H**) The output yield calculated from the plateau values of curves in (F) and (G), showing Output 1 (FAM) + Output 3 (HEX) = Constant. (**I** and **J**) The fluorescent curves of the circuit of (B) under the modification of Cap 5A, 5C (**I**) and Cap 5B, 5C (**J**). (**K**) The output yield calculated from the plateau values of curves in (I) and (J), showing Output 1 (FAM) = 2× Output 3 (HEX). Reaction set up: except for Caps, all other strands were fixed at 200 nM. The concentrations of Caps were determined according to the purpose of the experiment.

ways, selective activation and sliding rheostat. More importantly, all of the basic properties and advanced functions were fulfilled by the Cap strand alone, without changing the sequence design and structure of the original toehold-mediated reactions at all. Finally, combining all the regulatory functions of Cap and its distinct advantage of working independently, we achieved personalized tailor-made post-modification on packaged pre-fabricated DNA circuits. A pre-fabricated dual-output DNA circuit was successfully transformed to an equal-output circuit, a signal-antagonist circuit and a covariant circuit according to our wishes.

Overall, the sequence design of our proposed Cap is very simple and does not change the original sequences at all, making the tool general for all strand displacement-based DNA nanodevices. With the boom in development of packaged and batched DNA nanodevices, we believe the proposed Cap tool will be widely used in regulating reaction networks and personalized tailor-made modification of pre-fabricated DNA nanodevices.

DATA AVAILABILITY

The data underlying this article will be shared on reasonable request to the corresponding author.

SUPPLEMENTARY DATA

Supplementary Data are available at NAR Online.

ACKNOWLEDGEMENTS

Author contributions: L.Y.W., H.H. and T.X.F. designed the overall research strategy, and coordinated data collection and manuscript writing. X.X.J., M.Z.H. and L.L.J. were the lead researchers for conceptualization of the project, data analysis and manuscript writing. Q.Y., Z.W., D.K.J., Y.B. and M.Y.Q. participated in the related experiments. All authors were involved in the preparation of the final manuscript.

FUNDING

This work was financially supported by the National Natural Science Foundation of China [81871732]; the National Key Research and Development Program of China [2021YFC2701402]; the Open Research Fund of State Key Laboratory of Bioelectronics, South-east University [Sklb2021-k06]; the Open Foundation of NHC Key Laboratory of Birth Defect for Research and Prevention (Hunan Provincial Maternal and Child Health Care Hospital) [KF2020007]; and the Open Foundation of Translational Medicine National Science and Technology Infrastructure (Shanghai) [TMSK-2021-141].
Conflict of interest statement. None declared.

REFERENCES

1. Takahashi,S. and Sugimoto,N. (2021) Watson–Crick versus Hoogsteen base pairs: chemical strategy to encode and express genetic information in life. *Acc. Chem. Res.*, **54**, 2110–2120.
2. Li,J., Johnson-Buck,A., Yang,Y.R., Shih,W.M., Yan,H. and Walter,N.G. (2018) Exploring the speed limit of toehold exchange with a cartwheeling DNA acrobat. *Nat. Nanotechnol.*, **13**, 723–729.
3. Bath,J. and Turberfield,A.J. (2007) DNA nanomachines. *Nat. Nanotechnol.*, **2**, 275–284.
4. Woods,D., Doty,D., Myhrvold,C., Hui,J., Zhou,F., Yin,P. and Winfree,E. (2019) Diverse and robust molecular algorithms using reprogrammable DNA self-assembly. *Nature*, **572**, E21.
5. Blanchard,A.T. and Salaita,K. (2019) Emerging uses of DNA mechanical devices. *Science*, **365**, 1080–1081.
6. Yurke,B., Turberfield,A.J., Mills,A.P., Simmel,F.C. and Neumann,J.L. (2000) A DNA-fuelled molecular machine made of DNA. *Nature*, **406**, 605–608.
7. Yan,H., Zhang,X.P., Shen,Z.Y. and Seeman,N.C. (2002) A robust DNA mechanical device controlled by hybridization topology. *Nature*, **415**, 62–65.
8. Srinivas,N., Parkin,J., Seelig,G., Winfree,E. and Soloveichile,D. (2017) Enzyme-free nucleic acid dynamical systems. *Science*, **358**, eaal2052.
9. Arora,A.A. and de Silva,C. (2018) Beyond the smiley face: applications of structural DNA nanotechnology. *Nano Rev. Exp.*, **9**, 1430976.
10. Simmel,S.S., Nickels,P.C. and Liedl,T. (2014) Wireframe and tensegrity DNA nanostructures. *Acc. Chem. Res.*, **47**, 1691–1699.
11. Ouldridge,T.E., Louis,A.A. and Doye,J.P.K. (2011) Structural, mechanical, and thermodynamic properties of a coarse-grained DNA model. *J. Chem. Phys.*, **134**, 085101.
12. Zhang,D.Y. and Winfree,E. (2009) Control of DNA strand displacement kinetics using toehold exchange. *J. Am. Chem. Soc.*, **131**, 17303–17314.
13. Chen,X., Liu,N., Liu,L.Q., Chen,W., Chen,N., Lin,M., Xu,J.J., Zhou,X., Wang,H.B., Zhao,M.P. *et al.* (2019) Thermodynamics and kinetics guided probe design for uniformly sensitive and specific DNA hybridization without optimization. *Nat. Commun.*, **10**, 4675.
14. Beattie,K.L., Wiegand,R.C. and Radding,C.M. (1977) Uptake of homologous single-stranded fragments by superhelical DNA. II. Characterization of the reaction. *J. Mol. Biol.*, **116**, 783–803.
15. Sun,W.Q., Mao,C.D., Liu,F.R. and Seeman,N.C. (1998) Sequence dependence of branch migratory minima. *J. Mol. Biol.*, **282**, 59–70.
16. Srinivas,N., Ouldridge,T.E., Sulc,P., Schaeffer,J.M., Yurke,B., Louis,A.A., Doye,J.P.K. and Winfree,E. (2013) On the biophysics and kinetics of toehold-mediated DNA strand displacement. *Nucleic Acids Res.*, **41**, 10641–10658.
17. Xing,Y.Z., Yang,Z.Q. and Liu,D.S. (2011) A responsive hidden toehold to enable controllable DNA strand displacement reactions. *Angew. Chem. Int. Edit.*, **50**, 11934–11936.
18. Xing,C., Chen,Z.Y., Dai,J.D., Zhou,J., Wang,L.P., Zhang,K.L., Yin,X.F., Lu,C.H. and Yang,H.H. (2020) Light-controlled, toehold-mediated logic circuit for assembly of DNA tiles. *ACS Appl. Mater. Interfaces*, **12**, 6336–6342.
19. Zhou,R., Hu,C., Jin,Y., Zhang,J., Du,H., Yang,P., Chen,J., Hou,X. and Cheng,N. (2020) Spatially constrained DNA nanomachines to accelerate kinetics in response to external input: design and bioanalysis. *Anal. Chem.*, **92**, 8909–8916.
20. Tang,W., Wang,H.M., Wang,D.Z., Zhao,Y., Li,N. and Liu,F. (2013) DNA tetraplexes-based toehold activation for controllable DNA strand displacement reactions. *J. Am. Chem. Soc.*, **135**, 13628–13631.
21. Kim,W.J., Akaike,T. and Maruyama,A. (2002) DNA strand exchange stimulated by spontaneous complex formation with cationic comb-type copolymer. *J. Am. Chem. Soc.*, **124**, 12676–12677.
22. Genot,A.J., Zhang,D.Y., Bath,J. and Turberfield,A.J. (2011) Remote toehold: a mechanism for flexible control of DNA hybridization kinetics. *J. Am. Chem. Soc.*, **133**, 2177–2182.
23. Yang,X.L., Tang,Y.N., Traynor,S.M. and Li,F. (2016) Regulation of DNA strand displacement using an allosteric DNA toehold. *J. Am. Chem. Soc.*, **138**, 14076–14082.
24. Li,L.J., Zhang,W.K., Tang,X.F., Li,Z.J., Wu,Y.Z. and Xiao,X.J. (2020) Fine and bidirectional regulation of toehold-mediated DNA strand displacement by a wedge-like DNA tool. *Chem. Commun.*, **56**, 8794–8797.
25. Liu,L.Q., Hu,Q.Y., Zhang,W.K., Li,W.H., Zhang,W., Ming,Z.H., Li,L.J., Chen,N., Wang,H.B. and Xiao,X.J. (2021) Multifunctional clip strand for the regulation of DNA strand displacement and construction of complex DNA nanodevices. *ACS Nano*, **15**, 11573–11584.
26. Weng,Z., Yu,H.Y., Luo,W., Guo,Y.C., Liu,Q., Zhang,L., Zhang,Z., Wang,T., Dai,L., Zhou,X. *et al.* (2022) Cooperative branch

migration: a mechanism for flexible control of DNA strand displacement. *ACS Nano*, **16**, 3135–3144.
27. He,L., Lu,D.Q., Liang,H., Xie,S.T., Luo,C., Hu,M.M., Xu,L.J., Zhang,X.B. and Tan,W.H. (2017) Fluorescence resonance energy transfer-based DNA tetrahedron nanotweezer for highly reliable detection of tumor-related mRNA in living cells. *ACS Nano*, **11**, 4060–4066.
28. Li,J., Hong,C.Y., Wu,S.X., Liang,H., Wang,L.P., Huang,G.M., Chen,X., Yang,H.H., Shangguan,D.H. and Tan,W.H. (2015) Facile phase transfer and surface biofunctionalization of hydrophobic nanoparticles using janus DNA tetrahedron nanostructures. *J. Am. Chem. Soc.*, **137**, 11210–11213.
29. Qian,L. and Winfree,E. (2011) Scaling up digital circuit computation with DNA strand displacement cascades. *Science*, **332**, 1196–1201.
30. Song,X. and Reif,J. (2019) Nucleic acid databases and molecular-scale computing. *ACS Nano*, **13**, 6256–6268.
31. Shimada,N., Saito,K., Miyata,T., Sato,H., Kobayashi,S. and Maruyama,A. (2018) DNA computing boosted by a cationic copolymer. *Adv. Funct. Mater.*, **28**, 1707406.
32. Zhou,C.Y., Geng,H.M., Wang,P.F. and Guo,C.L. (2020) Ten-input cube root logic computation with rational designed DNA nanoswitches coupled with DNA strand displacement process. *ACS Appl. Mater. Interfaces*, **12**, 2601–2606.
33. Moerman,P.G. and Schulman,R. (2020) DNA computation improves diagnostic workflows. *Nat. Nanotechnol.*, **15**, 626–627.
34. Fu,D., Shah,S., Song,T. and Reif,J. (2018) DNA-based analog computing. *Methods Mol. Biol.*, **1772**, 411–417.
35. Lapteva,A.P., Sarraf,N. and Qian,L. (2022) DNA strand-displacement temporal logic circuits. *J. Am. Chem. Soc.*, **144**, 12443–12449.
36. Wu,Q., Liu,C.C., Liu,Y., Cui,C., Ge,J. and Tan,W.H. (2022) Multibranched linear DNA-controlled assembly of silver nanoclusters and their applications in aptamer-based cell recognition. *ACS Appl. Mater. Interfaces*, **14**, 14953–14960.
37. Hu,Q.Q., Li,H., Wang,L.H., Gu,H.Z. and Fan,C.H. (2019) DNA nanotechnology-enabled drug delivery systems. *Chem. Rev.*, **119**, 6459–6506.
38. Mo,F.L., Jiang,K., Zhao,D., Wang,Y.Q., Song,J. and Tan,W.H. (2021) DNA hydrogel-based gene editing and drug delivery systems. *Adv. Drug Deliv. Rev.*, **168**, 79–98.
39. Kim,J., Jang,D., Park,H., Jung,S., Kim,D.H. and Kim,W.J. (2018) Functional-DNA-driven dynamic nanoconstructs for biomolecule capture and drug delivery. *Adv. Mater.*, **30**, e1707351.
40. Tang,X.F., Chen,X., Liao,Y.W., Yan,B., Hu,H., Ming,Z.H., Liu,L.Q., Li,L.J., Mao,Z.H. and Xiao,X.J. (2021) Self-internal-reference probe system for control-free quantification of mutation abundance. *Anal. Chem.*, **93**, 13274–13283.
41. Ren,L.D., Ming,Z.H., Zhang,W., Liao,Y.W., Tang,X.F., Yan,B., Lv,H.M. and Xiao,X.J. (2022) Shared-probe system: an accurate, low-cost and general enzyme-assisted DNA probe system for detection of genetic mutation. *Chinese Chem. Lett.*, **33**, 3043–3048.
42. Zhang,W., Liu,L.Q., Liao,Y.W., Shu,W., Tang,X.F., Dong,K.J., Ming,Z.H., Xiao,X.J. and Wang,H.B. (2022) Thermodynamics-guided two-way interlocking DNA cascade system for universal multiplexed mutation detection. *Chinese Chem. Lett.*, **33**, 334–338.
43. Li,L., Xu,S.J., Yan,H., Li,X.W., Yazd,H.S., Li,X., Huang,T., Cui,C., Jiang,J.H. and Tan,W.H. (2021) Nucleic acid aptamers for molecular diagnostics and therapeutics: advances and perspectives. *Angew. Chem. Int. Edit.*, **60**, 2221–2231.
44. Bozza,M., De Roia,A., Correia,M.P., Berger,A., Tuch,A., Schmidt,A., Zornig,I., Jager,D., Schmidt,P. and Harbottle,R.P. (2021) A nonviral, nonintegrating DNA nanovector platform for the safe, rapid, and persistent manufacture of recombinant T cells. *Sci. Adv.*, **7**, eabf1333.
45. Jiang,Q., Zhao,S., Liu,J.B., Song,L.L., Wang,Z.G. and Ding,B.Q. (2019) Rationally designed DNA-based nanocarriers. *Adv. Drug Deliv. Rev.*, **147**, 2–21.